Frontiers in Bioscience Landmark

*Front. Biosci. (Landmark Ed)* **2023**; 28(12): 354
https://doi.org/10.31083/j.fbl2812354

*Original Research*

# Effects of Purine Metabolism-Related *LINC01671* on Tumor Heterogeneity in Kidney Renal Clear Cell Carcinoma

Wei Yin[1], Jin-Hua Wang[2], Yu-Mei Liang[1], Kang-Han Liu[1], Ying Chen[1], Yu-Sa Chen[3,4,5,*]

[1]Department of Nephrology, Hunan Provincial People's Hospital, The First Affiliated Hospital of Hunan Normal University, 410005 Changsha, Hunan, China
[2]Department of Nephrology, The First Affiliated Hospital of Hunan Normal University, 410005 Changsha, Hunan, China
[3]Nephrology Department and Laboratory of Kidney Disease, Hunan Provincial People's Hospital, The First Affiliated Hospital of Hunan Normal University, 410005 Changsha, Hunan, China
[4]Department of Nephrology, Changsha Clinical Research Center for Kidney Disease, 410002 Changsha, Hunan, China
[5]Department of Nephrology, Hunan Clinical Research Center for Chronic Kidney Disease, 410002 Changsha, Hunan, China
*Correspondence: chenyusa117@126.com (Yu-Sa Chen)
Academic Editor: Balachandran Manavalan
Submitted: 24 July 2023 Revised: 14 September 2023 Accepted: 20 September 2023 Published: 27 December 2023

**Abstract**

**Background**: Renal cell carcinoma has several subtypes, with kidney renal clear cell carcinoma (KIRC) being the most common and heterogeneous. Purine metabolism is associated with cancer progression. However, the role of purine metabolism-related long non-coding RNAs (lncRNAs) in KIRC remains unknown. **Methods**: KIRC were grouped into Cluster-1 and Cluster-2 based on purine genes. Limma package was used to identify differentially expressed lncRNAs between two classes of purine genes. Single-factor screening was used followed by random forest dimensionality reduction and Lasso method to screen lncRNAs. A risk score model (Purine Score) containing the 3 lncRNAs was developed using the Lasso method. **Results**: A total of 22 differentially expressed lncRNAs were identified. These were reduced to a final set of three (*LINC01671*, *ARAP1-AS1* and *LINC02747*). Age and metastasis (M) were identified as independent prognostic factors for KIRC using univariate and multivariate Cox analysis. An abnormal immune cell response was also associated with patient survival. The Purine Score correlated with abnormal expression of immune checkpoint genes. Genetic analysis of KIRC found somatic mutations in *TP53*, *TRIOBP*, *PBRM1*, *PKHD1*, *VHL*, *NPHP3*, *TLN2*, *CABIN1*, *ABCC6*, *XIRP2*, and *CHD4*. *In vitro* cell experiments showed that knockdown of *LINC01671* promoted the proliferation and migration of 786-O cells, while inhibiting apoptosis. Overexpression of *LINC01671* inhibited the proliferation and migration of CAKI-1 cells, while promoting apoptosis. Gene Set Enrichment Analysis (GSEA) analysis revealed that *LINC01671* was significantly enriched in the MAPK, NF-kappa B, mTOR, PI3K-Akt, and Wnt signaling pathways. **Conclusions**: *LINC01671* may be a novel prognostic marker with important therapeutic value for KIRC.

**Keywords:** purine metabolism; *LINC01671*; tumor heterogeneity; kidney renal clear cell carcinoma

## 1. Introduction

Kidney epithelium is the site of origin of renal cell carcinoma (RCC), which accounts for around 90% of all kidney cancers [1]. The most prevalent subtype of RCC is kidney renal clear cell carcinoma (KIRC) [2], characterized by a high cytoplasmic lipid content and considered to be a metabolic cancer [3]. KIRC is a highly metastatic and recurrent malignant renal tumor associated with high morbidity and mortality [4], and has become a major health problem worldwide [5]. This cancer type is characterized by mutations in genes that control the hypoxia signaling pathway, thus leading to metabolic imbalance, enhanced angiogenesis, intra-tumoral heterogeneity, and a harmful tumor microenvironment (TME) [6]. KIRC also interacts with the TME, which helps to guide appropriate treatment [7]. It is therefore imperative to achieve a comprehensive understanding of the molecular mechanisms that underlie KIRC and to devise effective strategies for its timely diagnosis and treatment.

The reprogramming of energy metabolism is a hallmark of cancer that has recently gained special attention due to its promotion of cell growth and proliferation [8]. Purine is a vital substrate in organisms and serves as a crucial material for cell proliferation and important factor in immune regulation [9]. It is also an essential component of various cellular processes, including energy metabolism, cell signaling, and the encoding of genetic material [10]. The final product of purine metabolism in humans, uric acid, has potent antioxidant properties [11]. Dysfunction of purine metabolism has serious physiological and pathological consequences [12], and impaired purine metabolism is associated with cancer progression [13]. Jackson RC *et al.* [14] were the first to describe the involvement of purine metabolism enzymes in the renal cortex and kidney cells of RCC in humans and rats. However, the role of purine metabolism in KIRC is not yet fully understood.

Long non-coding RNAs (lncRNAs) are RNA transcripts >200 nucleotides in length that bind to DNA, RNA

and proteins [15] and are thus capable of modulating cellular physiology and function. Disruption of lncRNA expression or function is closely associated with various inherited, autoimmune and metabolic diseases, as well as tumors [16]. The overexpression of oncogenic lncRNAs and reduction of tumor suppressor lncRNAs are common features of human RCC. Abnormal expression of lncRNAs is a crucial factor in RCC progression and an indicator of poor prognosis for these patients [17]. The role in KIRC of lncRNAs related to purine metabolism has yet to be determined.

With the above background in mind, we performed non-negative matrix factorization (NMF) clustering to classify KIRC and identify purine-related patterns. We developed a purine-related, differential lncRNA risk score (Purine Score) to predict the outcome of KIRC patients. We also conducted analyses of immune cell infiltration, immune checkpoint expression, and gene mutation. Finally, we carried out preliminary *in vitro* cell experiments to validate the function of purine metabolism-related differential lncRNAs. Characterization of these lncRNAs could help to guide the development of more personalized treatment strategies for KIRC.

## 2. Materials and Methods

### *2.1 Dataset and Preprocessing*

The dataset for KIRC was downloaded from The Cancer Genome Atlas (TCGA) located at UCSC Xena (https://xenabrowser.net/). RNA sequencing (RNA-seq) data was extracted from the TCGA data portal. Values for fragments per kilobase million (FPKM) were converted to transcripts per million (TPM).

### *2.2 Clustering of Purine Genes in KIRC*

A total of 130 purine-related genes were obtained from KEGG (hsa00230; purine metabolism), and 129 overlapping genes were identified by intersecting with the TCGA gene set. Single-factor Cox filtering was used to identify 65 genes with $p < 0.01$. NMF clustering was used to classify KIRC and to identify purine-related patterns, with the patients then grouped for subsequent analysis.

### *2.3 Development of a Purine-Related LncRNA Risk Score*

The limma package (version 3.56.2, https://bioinf.wehi.edu.au/limma/) was employed for single-factor filtering and to identify differentially expressed lncRNAs in the purine-associated category, using a significance threshold of $p < 0.05$ and $|\log FC| > 1$. Random survival forest was then used to perform further screening, and the Lasso method was employed to build a model using the selected genes. The risk score was calculated by multiplying gene expression values with the regression coefficients. The surv_cutpoint function of the survminer package (version 0.4.9, https://rpkgs.datanovia.com/survminer/index.html) was then applied to classify patients into high- and low-risk groups. The timeROC R package (version 0.4, https://www.rdocumentation.org/packages/timeROC/versions/0.4) was used to plot time-ROC curves.

### *2.4 Immune Cell Infiltration and Pathway Analysis*

The MCPcounter and TIMER algorithms were utilized to evaluate immune cell abundance in KIRC samples and to identify disparities in immune cell infiltration across distinct clustering categories or risk groups. Gene Set Enrichment Analysis (GSEA) was performed to examine KEGG pathway regulation. The maftools R package (version 2.16.0, https://github.com/PoisonAlien/maftools) was used for mutation analysis.

### *2.5 Cell Culture and Treatments*

The cells of the human RCC line 786-O (AW-CCH060) and CAKI-1 (AW-CCH173) were purchased from Abiowell (Changsha, Hunan, China). 786-O or CAKI-1 cells were cultured in RPMI-1640 or McCoy's 5A medium containing 10% fetal bovine serum and 1% Penicillin/Streptomycin. All cells were maintained at 37 °C with 5% $CO_2$ in a humidified atmosphere. All cell lines have been authenticated in the past three years. All cell lines were identified by STR profile. All experiments were performed with mycoplasma-free cells. Both knockdown and overexpression of *LINC01671* were performed. 786-O cells were divided into control, sh-NC, and sh-*LINC01671* groups, and CAKI-1 cells into control, oe-NC, and oe-*LINC01671* groups. The sh-*LINC01671*, oe-*LINC01671*, and negative controls (sh-NC and oe-NC) were provided by HonroGene (Changsha, Hunan, China). All transfections were performed using Lipofectamine 2000 (11668019, Invitrogen, Waltham, MA, USA).

### *2.6 Quantitative Real-Time PCR (qRT-PCR)*

qRT-PCR was utilized to evaluate *LINC01671*, *ARAP1-AS1*, and *LINC02747* levels. Total RNA was extracted and reverse transcribed into cDNAs. Ultra SYBR Mixture (CW2601, CWBIO, Cambridge, MA, USA) was used to test on the ABI 7900 system. Gene expression was calculated using the $2^{-\Delta\Delta Ct}$ method, with *GAPDH* as the internal reference. Primer sequences were: *LINC01671*-F: TCAGGAACACCTCACAGGTC, *LINC01671*-R: GCAAACTCCAAGAGGAGTCCA; *ARAP1-AS1*-F: TCCTCTACAGCACCCGCTTT, *ARAP1-AS1*-R: CCACCCTTTCAGAGGCGTGAG; *LINC02747*-F: GAAGATGTGCACCTGCCGAG, *LINC02747*-R: GGTTGAGTTCAATGGCAGCA; *GAPDH*-F: ACAGCCTCAAGATCATCAGC, *GAPDH*-R: GGTCATGAGTCCTTCCACGAT.

### *2.7 Cell Counting Kit 8 (CCK-8) Assay*

Cells were seeded at a density of $1 \times 10^4$/100 µL in a 96-well plate and incubated at 37 °C in 5% $CO_2$. After adding 10 µL CCK-8 (NU679, DOJINDO, Tokyo, Japan),

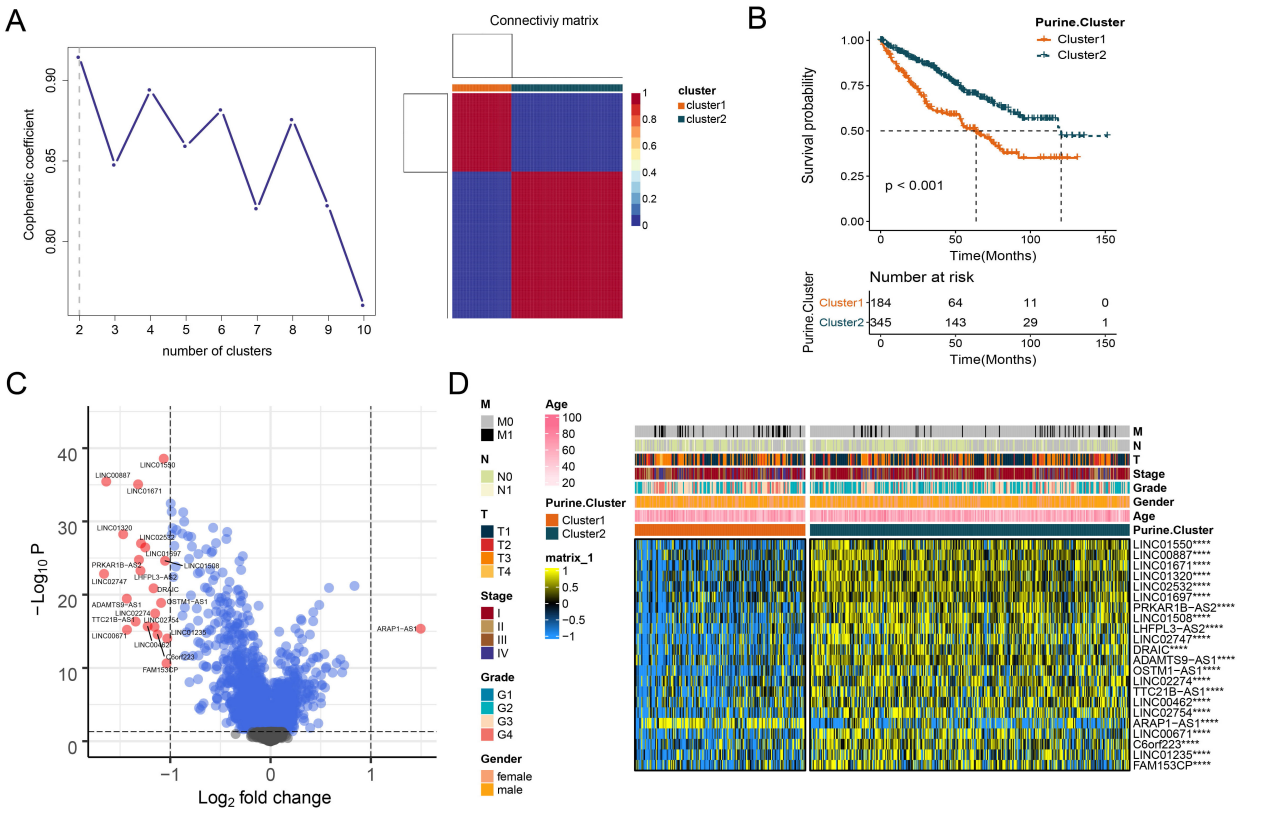


**Fig. 1. Clustering of kidney renal clear cell carcinoma (KIRC) based on purine genes.** (A) Non-negative matrix factorization (NMF) clustering analysis. (B) Survival analysis for Cluster-1 and Cluster-2. (C) Differentially expressed long non-coding RNAs (lncRNAs) between Cluster-1 and Cluster-2 were visualized by a volcano plot. (D) Clustering heatmap showing the expression of purine-related lncRNAs in Cluster-1 and Cluster-2. M, Metastasis; N, Node; T, Tumor. ****$p < 0.0001$.

cells were incubated at 37 °C in 5% $CO_2$ for 4 h. Optical density (OD) values for absorbance at 450 nm were analyzed using an enzyme marker (MB-530, Heales, Shenzhen, Guangdong, China).

### *2.8 Cell Migration Assay*

Cells were suspended in serum-free medium at $1 \times 10^6$/mL and 100 µL was added to the upper chamber of a Transwell (33318035, Corning, Somerville, MA, USA). The lower chamber was filled with complete medium containing 10% fetal bovine serum (FBS). After removal of the culture medium from the upper chamber, the upper surface of cells was wiped with a wet cotton swab. The cells were then fixed and stained with crystal violet. Cells on the outer surface of the upper chamber were observed and photographed under a microscope (Olympus, Tokyo, Japan).

### *2.9 Flow Cytometry*

Cells were digested and centrifuged, and about $3.2 \times 10^5$ cells were collected. These were suspended in 500 µL of binding buffer, and 5 µL allophycocyanin (APC) and propidium iodide were added and mixed. Reaction was carried out in the dark, and the cells analyzed by flow cytometry (A00-1-1102, Beckman, Pasadena, CA, USA) within 1 h.

### *2.10 Terminal Deoxynucleotidyl Transferase Mediated dUTP Nick-End Labeling (TUNEL)*

A TUNEL apoptosis detection kit (FITC) (40306ES50, Yeasen, Shanghai, China) was used to evaluate cell apoptosis. After fixation, cells were permeabilized with Triton X-100 and sodium citrate solution, and then treated with fluorescent-labeled nucleotides (dUTP) and TdT. TUNEL-positive cells with green fluorescence were observed and quantified with a fluorescence microscope.

### *2.11 Statistical Analysis*

Normative variables were tested using the Shapiro-Wilk test, while normally distributed variables were compared with unpaired Student's *t*-test. Non-normally distributed variables were compared using the Wilcoxon test. One-way analysis of variance (ANOVA) was used as a parametric method to compare multiple groups, and the Kruskal-Wallis test as a non-parametric method. For each dataset, patients were categorized by binary risk score, with the R package ggplot2 (version 3.4.3, https://ggplot2.tidyverse.org/) used to visualize data. The Benjamini-Hochberg method was used to analyze differential gene expression. Significant genes were identified via

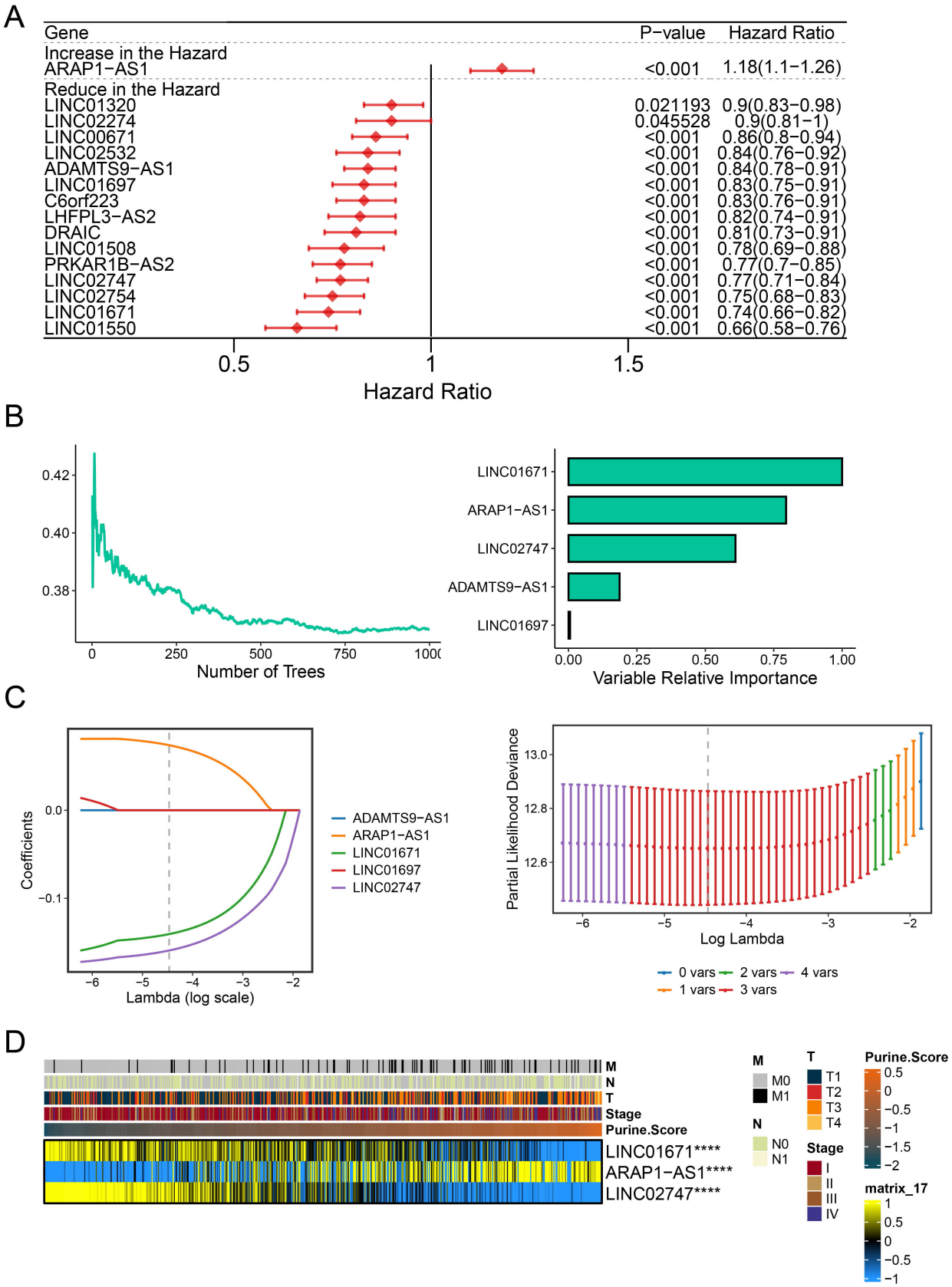


**Fig. 2. Development of a risk score (Purine Score) based on differentially expressed, purine-related lncRNAs.** (A) Univariate Cox analysis identified 16 purine-related lncRNAs. (B) Random forest analysis identified 5 lncRNAs. (C) Lasso analysis identified 3 lncRNAs. (D) Clustering heatmap used to visualize expression of 3 lncRNAs. ****$p < 0.0001$.

**Table 1. Sixty-five genes were selected by univariate Cox analysis.**

| Gene | Hazard Ratio (HR) | *p* value |
|---|---|---|
| *ADA* | 1.322225732 | 0.000141 |
| *NME6* | 0.615467044 | 0.004376 |
| *AK6* | 0.669127204 | 0.005059 |
| *ADCY1* | 0.574498565 | 0.000207 |
| *ADCY2* | 0.75597765 | 0.000395 |
| *ADCY5* | 0.685391664 | 0 |
| *NUDT5* | 1.626416449 | 0.000811 |
| *ADCY9* | 0.598294779 | 0 |
| *AK7* | 0.569865374 | $3.00 \times 10^{-6}$ |
| *NUDT16* | 0.605200248 | $8.90 \times 10^{-5}$ |
| *ADK* | 0.601568642 | $3.80 \times 10^{-5}$ |
| *ADSL* | 0.640166167 | 0.00343 |
| *AK8* | 0.596918634 | $5.90 \times 10^{-5}$ |
| *DCK* | 0.692206957 | 0.000238 |
| *DGUOK* | 1.86004424 | 0.002658 |
| *AK2* | 0.542739757 | $2.30 \times 10^{-5}$ |
| *AK4* | 0.863904135 | 0.006743 |
| *AK9* | 0.664702673 | 0.005243 |
| *ENPP4* | 0.593929734 | 0 |
| *AMPD2* | 1.383331903 | 0.009987 |
| *PDE7B* | 0.592125813 | 0 |
| *GUCY1A1* | 0.787063349 | $5.00 \times 10^{-5}$ |
| *NUDT2* | 0.58149016 | $1.20 \times 10^{-5}$ |
| *IMPDH1* | 1.926126267 | 0 |
| *ITPA* | 1.991948966 | 0.000175 |
| *ENTPD8* | 0.615480519 | 0.006383 |
| *ATIC* | 1.478253406 | 0.00086 |
| *NME1* | 1.728680516 | $1.00 \times 10^{-6}$ |
| *NME2* | 2.03014889 | $2.00 \times 10^{-6}$ |
| *NME3* | 1.42570392 | 0.00202 |
| *NME4* | 1.788156728 | 0 |
| *PNP* | 0.655616998 | $5.00 \times 10^{-6}$ |
| *NPR2* | 1.798747676 | 0 |
| *NT5E* | 0.819514456 | 0.008668 |
| *RRM2B* | 0.679064066 | $4.20 \times 10^{-5}$ |
| *AK3* | 0.588356084 | 0 |
| *GMPR2* | 0.476951021 | 0 |
| *PDE1C* | 0.710323592 | 0.001792 |
| *PDE2A* | 0.70866223 | 0 |
| *PDE3A* | 0.801720547 | 0.009234 |
| *PDE4D* | 0.535287823 | 0 |
| *PDE9A* | 0.709025554 | 0.000394 |
| *PDE6B* | 0.823131936 | 0.003545 |
| *ENPP3* | 0.901450829 | 0.002451 |
| *ADA2* | 0.836659234 | 0.009229 |
| *PGM1* | 0.720722714 | 0.000803 |
| *PKLR* | 0.804793889 | $8.00 \times 10^{-6}$ |
| *PKM* | 0.701745057 | 0.004423 |
| *NUDT9* | 0.614848462 | $4.50 \times 10^{-5}$ |
| *PPAT* | 0.717877922 | 0.005324 |
| *PGM2* | 0.641367057 | 0 |
| *PRPS1* | 0.714070279 | 0.001607 |
| *PRPS2* | 0.715145179 | 0.002363 |
| *ADPRM* | 0.576786343 | 0.000419 |
| *RRM1* | 0.72659287 | 0.006432 |
| *RRM2* | 1.371503543 | $4.80 \times 10^{-5}$ |
| *NTPCR* | 0.686055101 | 0.004177 |
| *PDE5A* | 0.774305725 | 0.007502 |
| *PAPSS1* | 0.662694715 | 0.000202 |
| *NT5C1B* | 0.274690557 | 0.003612 |
| *ENTPD1* | 0.755673824 | 0.000805 |
| *ENTPD2* | 0.72814631 | $7.00 \times 10^{-6}$ |
| *ENTPD6* | 1.671090139 | 0.000499 |
| *ENTPD5* | 0.705890706 | $1.00 \times 10^{-6}$ |
| *GDA* | 0.813727989 | $3.10 \times 10^{-5}$ |

the conversion of *p*-values to false discovery rate (FDR). The Kaplan-Meier method was used to compare survival of different patient groups, with the logarithmic rank test used to assess whether differences were statistically significant. All survival curves were generated using the R package survminer, and all heatmaps using pheatmap. Statistical analysis was performed using R (version 3.6.1, https://www.r-project.org/), with statistical significance set at $p < 0.05$ for two-sided tests.

## 3. Results

### *3.1 Clustering of KIRC Based on Purine Genes*

A total of 130 purine-related genes (KEGG: hsa00230; purine metabolism) were identified from the literature. The intersection of these genes with TCGA resulted in 129 genes. Subsequently, 65 genes were selected by univariate Cox analysis ($p < 0.01$, Table 1). KIRC were grouped into Cluster-1 and Cluster-2 according to purine genes. As the number of clusters increased, the cophenetic coefficient decreased (Fig. 1A). Survival analysis showed that Cluster-2 patients had better survival than Cluster-1 patients (Fig. 1B). A volcano plot was used to visualize differences in lncRNAs between the two clusters. The limma package identified 22 differentially expressed lncRNAs between Cluster-1 and Cluster-2 (Fig. 1C). A heatmap further visualized the expression of purine-related lncRNAs between the two clusters (Fig. 1D).

### *3.2 Development of a Risk Score (Purine Score) Based on Differentially Expressed, Purine-Related LncRNAs*

Purine-related lncRNAs were first screened by univariate Cox analysis (Fig. 2A). This identified *ARAP1-AS1* with an increased hazard ratio, and 15 lncRNAs with a decreased hazard ratio (*LINC01320*, *LINC02274*, *LINC00671*, *LINC02532*, *ADAMTS9-AS1*, *LINC01697*, *C6orf223*, *LHFPL3-AS2*, *DRAIC*,

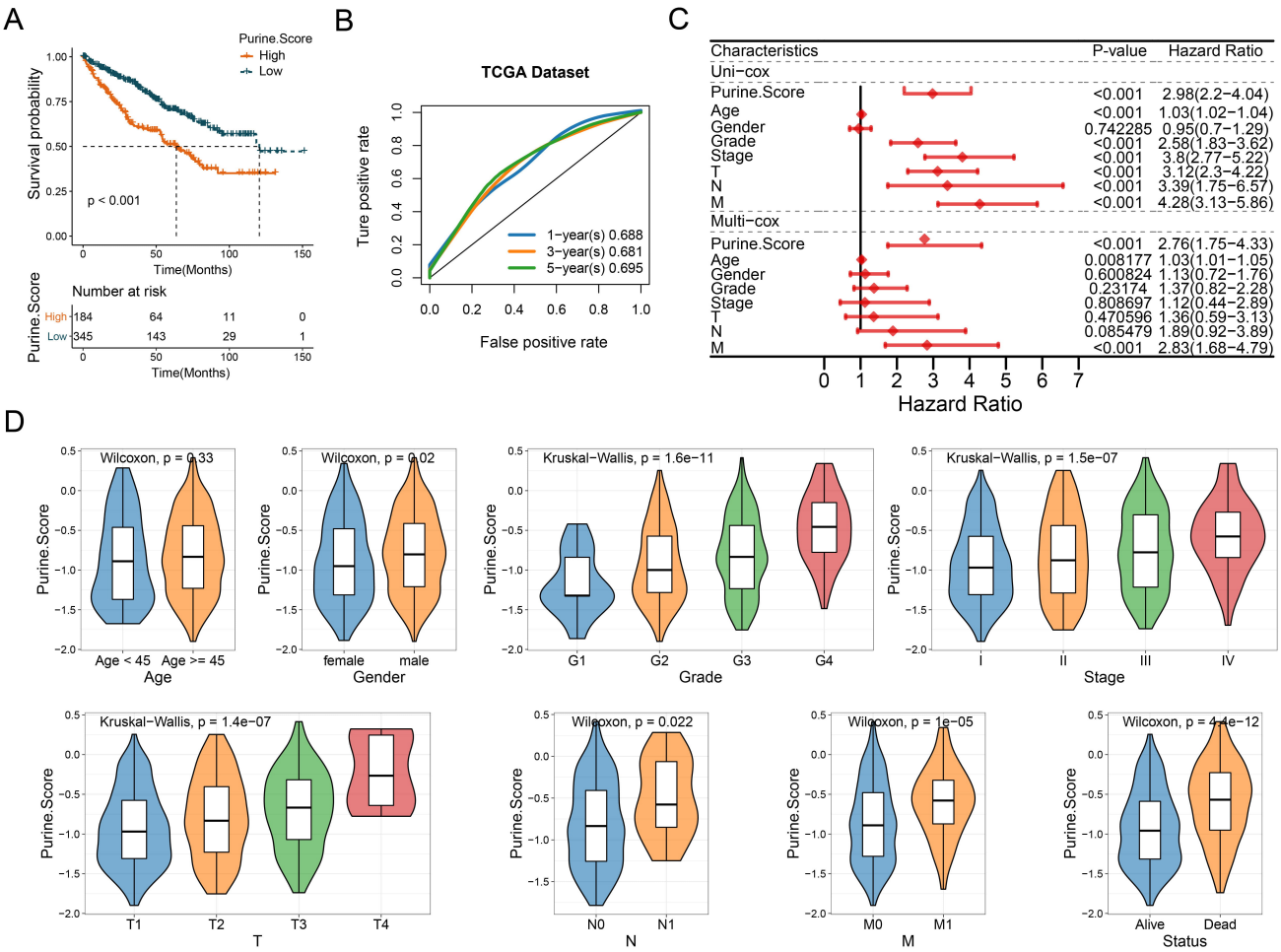


**Fig. 3. Prediction of outcome in KIRC patients using Purine Score.** (A) Survival analysis based on the risk score. (B) Receiver operating characteristic (ROC) analysis. (C) Identification of prognostic factors using univariate and multivariate Cox analyses. (D) Analysis of Purine Score according to clinical features. TCGA, The Cancer Genome Atlas.

*LINC01508*, *PRKARIB-AS2*, *LINC2747*, *LINC02754*, *LINC01671*, and *LINC01550*). Next, random forest analysis was used to reduce the dimension, resulting in 5 lncRNAs (*LINC01671*, *ARAP1-AS1*, *LINC02747*, *ADAMTS9-AS1*, and *LINC01697*; Fig. 2B). Lasso analysis then identified 3 lncRNAs (*LINC01671*, *ARAP1-AS1* and *LINC02747*; Fig. 2C). Finally, the Lasso method was used to obtain a risk score model comprised of 3 lncRNAs: $-0.1406 \times$ *LINC01671* $+ 0.0739 \times$ *ARAP1-AS1* $- 0.1592 \times$ *LINC02747*. A clustering heatmap was used to visualize expression of the 3 lncRNAs (*LINC01671*, *ARAP1-AS1*, and *LINC02747*; Fig. 2D).

### *3.3 Prediction of KIRC Patient Outcome Using Purine Score*

According to the risk score model established following TCGA survival analysis, patients with high risk scores had worse prognosis ($p < 0.05$, Fig. 3A). Moreover, based on receiver operating characteristic (ROC) analysis, the area under the curve (AUC) for Purine Score in TCGA were 0.688, 0.681, and 0.695 for 1-, 3-, and 5-year true-positive rates, respectively (Fig. 3B). We also investigated prognostic factors using univariate and multivariate Cox analyses. Age and metastasis (M) were found to be independent prognostic factors for KIRC patients (Fig. 3C). Finally, the Purine Score was evaluated according to various clinical features (Fig. 3D). Significant differences in the Purine Score were found according to gender, grade, stage, tumor (T), node (N) and status ($p < 0.05$).

### *3.4 Analysis of Immune Cell Infiltration and Immune Checkpoints*

Next, we performed a correlation analysis between prognosis and immune cell infiltration. As shown in Fig. 4A, the Purine Score correlated with cellular immune response and cell components, as determined by the MCPcounter and TIMER algorithms. The survival model included abnormalities in cytotoxic lymphocytes, NK cells, myeloid dendritic cells, monocytic lineage, endothelial cells, neutrophils, B cells, T cells CD4, neutrophils, macrophages, and DCs. Patients with a low Purine Score showed significantly higher scores for ESTIMATE ($p$

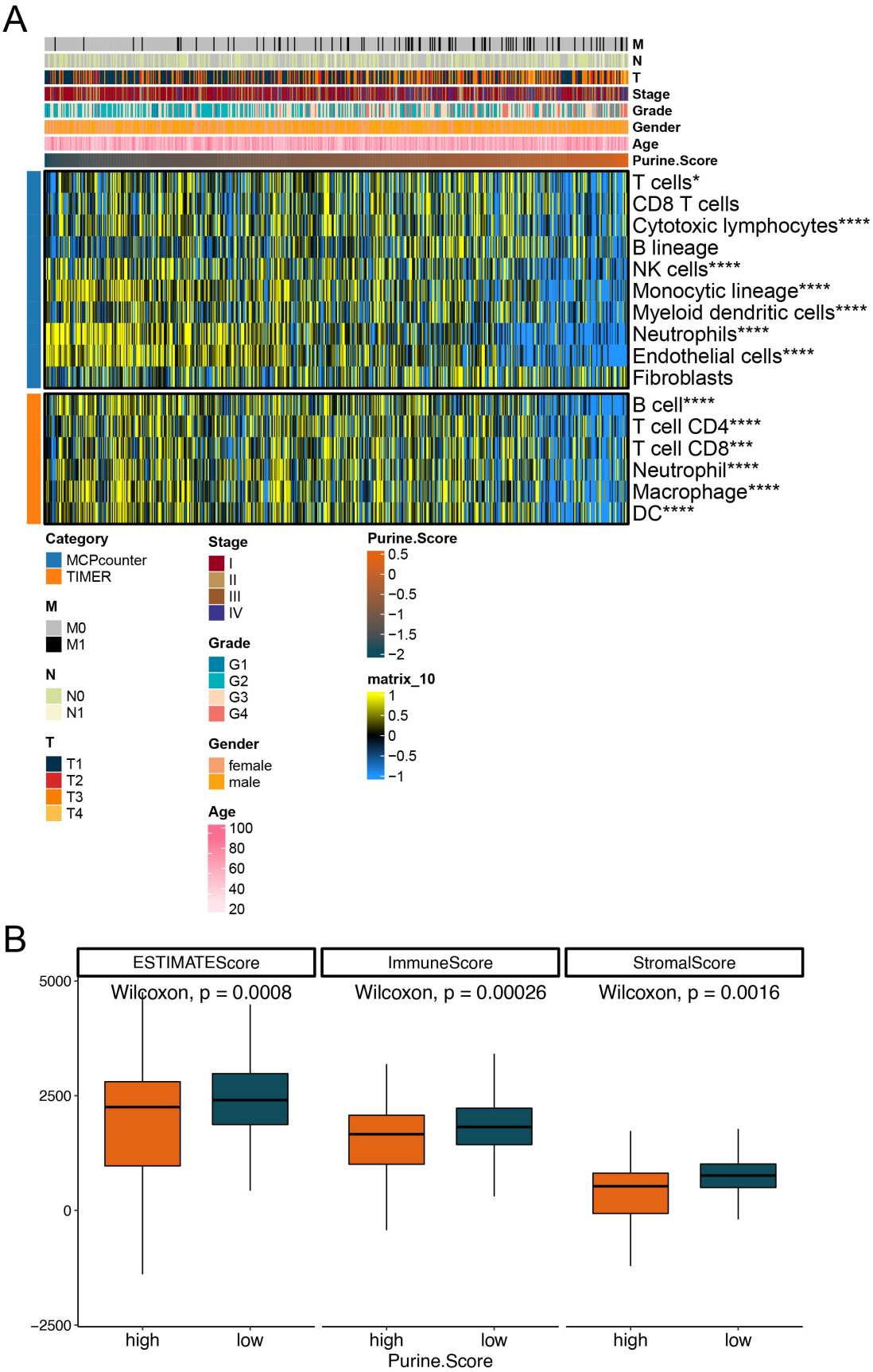


**Fig. 4. Analysis of immune cell infiltration and immune checkpoints.** (A) Analysis of immune cell infiltration. (B) ESTIMATE, Immune, and Stromal Scores. *$p < 0.05$, ****$p < 0.0001$.

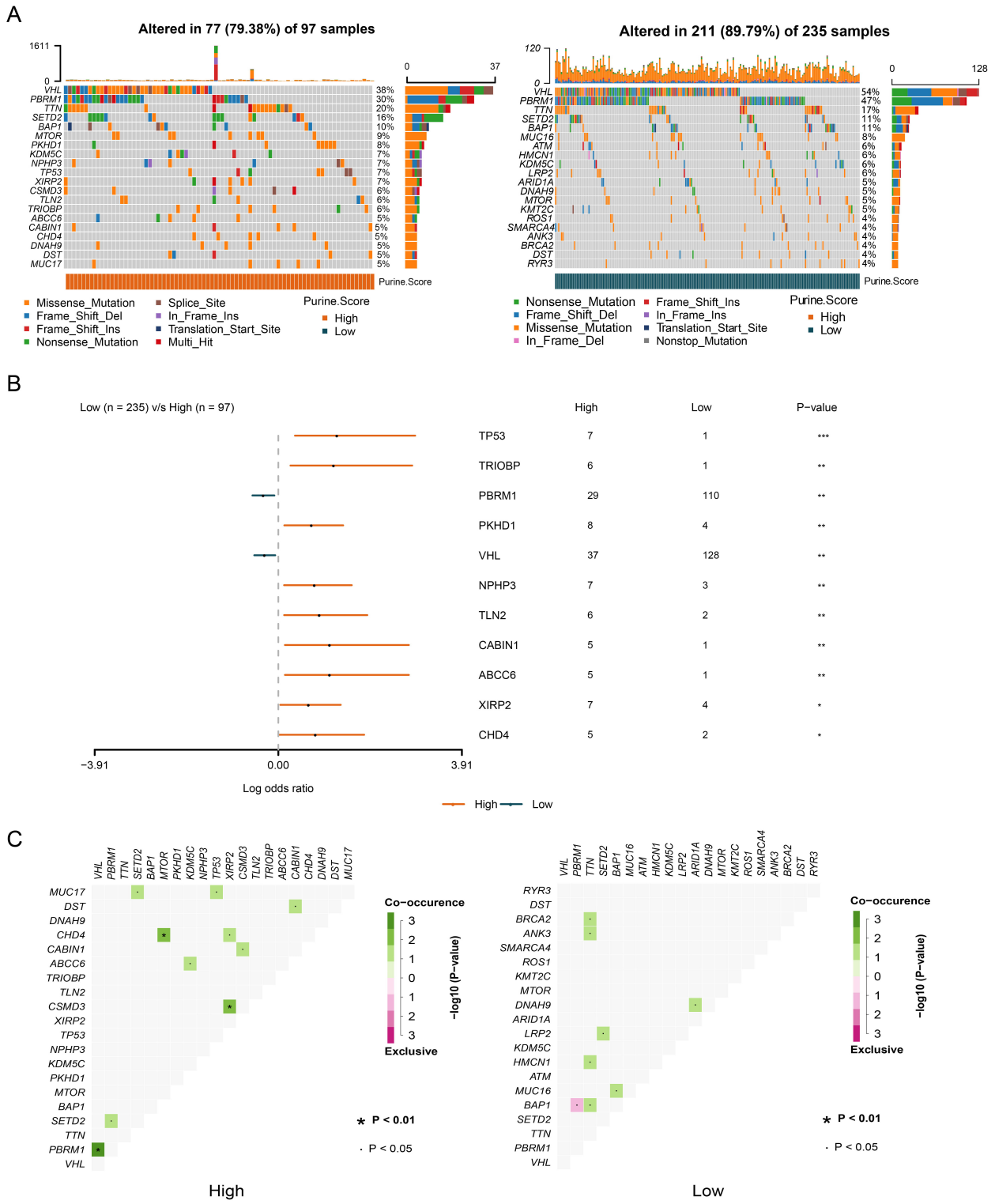


**Fig. 5. Analysis of gene mutations.** (A) Somatic mutation analysis. (B) Gene mutation frequencies in the high and low Purine Score groups. (C) Co-occurrence of mutated genes in the high and low Purine Score groups. ■$p < 0.05$, *$p < 0.01$.

= 0.0008), immune ($p = 0.00026$), and stromal ($p = 0.0016$) compared to patients with a high Purine Score (Fig. 4B). Correlation of immune regulation factors with the Purine Score are shown in **Supplementary Fig. 1**. The classification categories for immune checkpoints were cell adhesion, antigen presentation, co-stimulator, co-inhibitor, ligand, other, and receptor. A significant association was observed between the expression of immune checkpoint genes and the Purine Score.

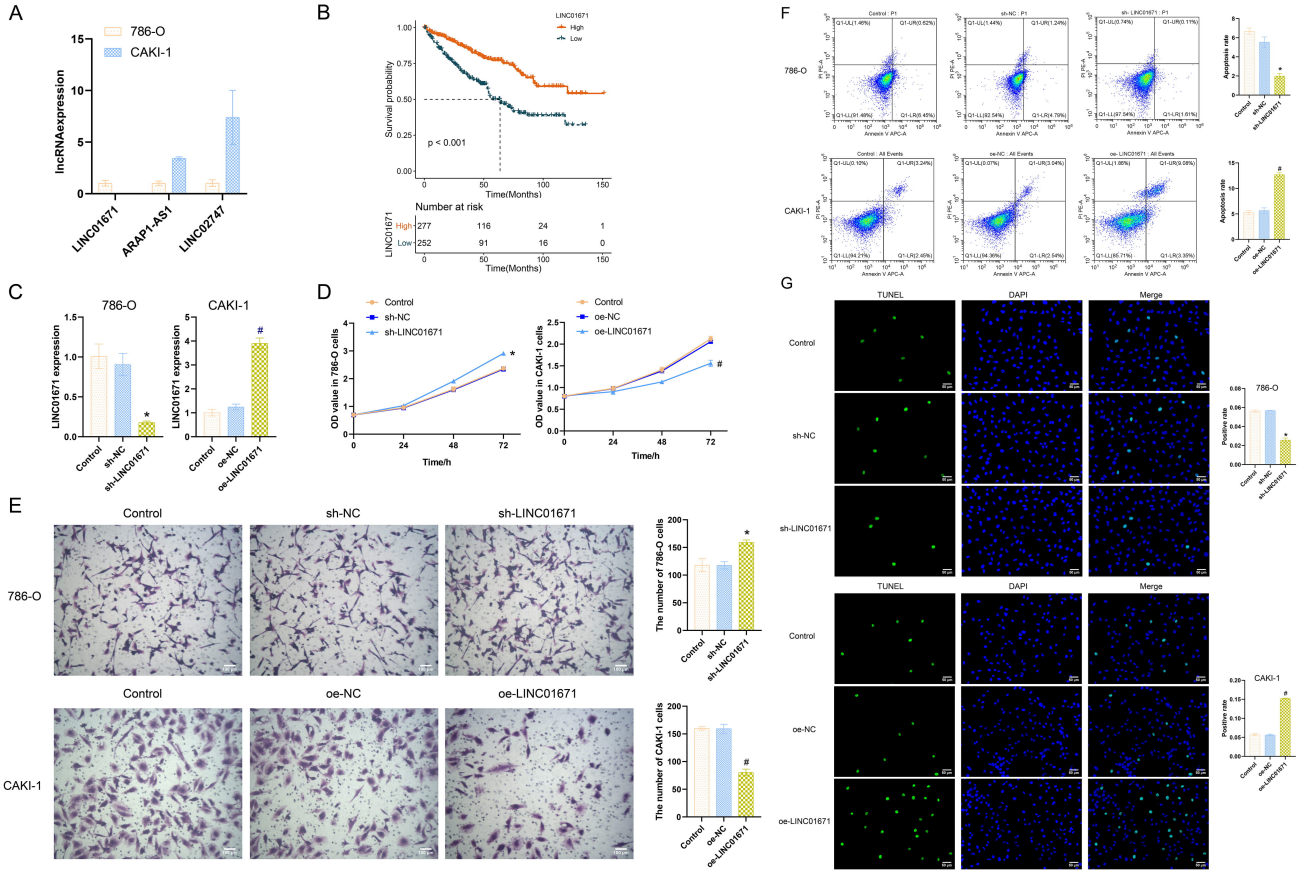


**Fig. 6. Validation of lncRNA expression.** (A) Quantitative real-time PCR (qRT-PCR) analysis of *LINC01671*, *ARAP1-AS1*, and *LINC02274* levels in 786-O and CAKI-1 cells. (B) Survival analysis according to *LINC01671* expression level. (C) qRT-PCR analysis of *LINC01671* expression after transfection of 786-O and CAKI-1 cells. (D) Cell counting kit 8 (CCK-8) assay results for cell proliferation. (E) Transwell cell migration results. (F) Flow cytometry analysis of cell apoptosis. (G) Terminal Deoxynucleotidyl Transferase mediated dUTP Nick-End Labeling (TUNEL) analysis of cell apoptosis. * $p < 0.05$ vs. sh-NC, # $p < 0.05$ vs. oe-NC.

### *3.5 Analysis of Gene Mutations*

Somatic mutation analysis revealed alterations in 77 of 97 (79.38%) KIRC with a high Purine Score (Missense Mutation, Frame Shift Del, Splice Site, Frame Shift Ins, In Frame Ins, Nonsense Mutation, Translation Start Site, and Multi Hit). Moreover, 211 of 235 (89.79%) KIRC with a low Purine Score showed alterations (Nonsense Mutation, Frame Shift Del, Frame Shift Ins, Missense Mutation, In Frame Ins, Translation Start Site, In Frame Del, and Nonstop Mutation, Fig. 5A). Gene mutation frequencies for the high and low Purine Score groups are shown in Fig. 5B. The mutation frequencies for *TP53*, *TRIOBP*, *PKHD1*, *NPHP3*, *TLN2*, *CABIN1*, *ABCC6*, *XIRP2*, and *CHD4* were significantly higher in the high Purine Score group compared to the low Purine Score group, whereas the mutation frequencies for *PBRM1* and *VHL* were significantly lower. Furthermore, in the high Purine Score group, *VHL* mutation co-occurred with *PBRM1* mutation, *PBRM1* with *SETD2*, *SETD2* with *MUC17*, *MTOR* with *CHD4*, *KDM5C* with *ABCC6*, *TP53* with *MUC17*, *XIRP2* with *CHD4* and *CSMD3*, *CSMD3* with *CABIN1*, and *CABIN1* with *DST*. In the low Purine Score group, *PBRM1* mutation did not co-occur with *BAP1*, *TTN* mutation co-occurred with *BRCA2*, *ANK3*, *HMCN1* and *BAP1* mutation, *SETD2* mutation co-occurred with *LRP2*, *BAP1* and *MUC16* mutation, and *ARID1A* with *DNAH9* (Fig. 5C).

### *3.6 Validation of LncRNA Expression*

Next, we used *in vitro* experiments to validate cell expression of the selected 3 lncRNAs (*LINC01671*, *ARAP1-AS1*, and *LINC02274*). qRT-PCR revealed high expression of *LINC01671* in 786-O cells, and low expression in CAKI-1 cells. Since *ARAP1-AS1* and *LINC02274* were highly expressed in both 786-O and CAKI-1 cell lines (Fig. 6A), *LINC01671* was therefore selected for further study. Survival analysis showed that high expression of *LINC01671* was associated with improved survival (Fig. 6B). Next, *LINC01671* was knocked down in 786-O cells and overexpressed in CAKI-1 cells. Successful transfection of sh-*LINC01671* and of oe-*LINC01671* was achieved, as shown in Fig. 6C. Cell function experiments showed that knockdown of *LINC01671* in 786-O cells promoted their prolif-

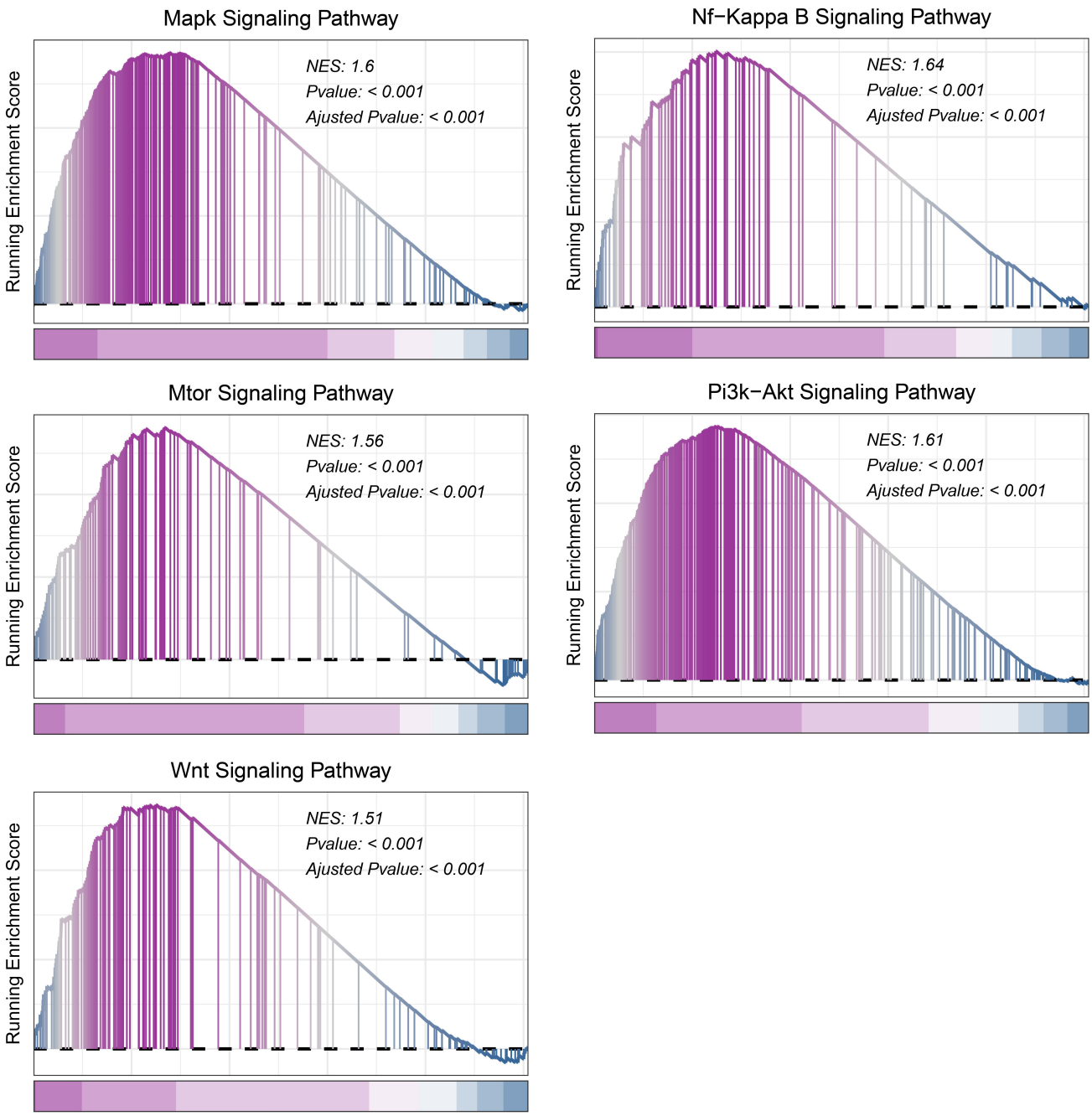


**Fig. 7. Functional enrichment analysis of *LINC01671*.** Gene Set Enrichment Analysis (GSEA) of the function and pathways for *LINC01671*.

eration and migration, but inhibited apoptosis. In contrast, overexpression of *LINC01671* in CAKI-1 cells inhibited their proliferation and migration, while promoting apoptosis (Fig. 6D–G).

### *3.7 Functional Enrichment Analysis of LINC01671*

Finally, we performed functional enrichment analysis of *LINC01671*. GSEA showed that *LINC01671* was mainly enriched in the MAPK (normalized enrichment score (NES) = 1.6, $p < 0.001$), NF-kappa B (NES = 1.64, $p < 0.001$), mTOR (NES = 1.56, $p < 0.001$), PI3K-Akt (NES = 1.61, $p < 0.001$) and Wnt (NES = 1.51, $p = 0.0001$) signaling pathways (Fig. 7). These results suggest that *LINC01671* may positively regulate the MAPK, NF-kappa B, mTOR, PI3K-Akt and Wnt signaling pathways. The flow chart is shown in **Supplementary Fig. 2**.

## 4. Discussion

KIRC is most common histological subtype of RCC and is more likely to metastasize, relapse, and resist radiotherapy and chemotherapy [18]. Various types of drug resistance can occur in KIRC due to the highly dynamic,

adaptable and heterogeneous nature of its TME, as well as to aberrant glucose and lipid metabolism [19,20]. Hence, there is an urgent need for non-invasive tools to accurately stratify and select patients for treatment. In the present study, we performed NMF clustering to develop a purine-related differential lncRNA risk score (Purine Score). We then analyzed immune cell infiltration, immune checkpoints and gene mutations in KIRC. Finally, we conducted *in vitro* experiments with KIRC cell lines to validate the function of purine metabolism-related differential lncRNAs. Our study found that purine metabolism-related *LINC01671* may be a key target for KIRC, thus affecting tumor heterogeneity.

Cancer cells undergo metabolic adaptation through multiple endogenous and exogenous signaling pathways. This enhances malignant cell growth and also initiates the transformative process of cell adaptation to the TME [21]. RCC is essentially a metabolic disease characterized by the reprogramming of energy metabolism [22–25]. In particular, the metabolic flux through glycolysis is partitioned [26–28], and mitochondrial bioenergetics, OxPhox and lipid metabolism are all impaired [26,29–31]. The translocation of metabolites related to the pentose phosphate pathway (PPP) are also known to be altered in RCC. The PPP supports key aspects of accelerated tumor growth and generates precursors for nucleotide synthesis. The "Warburg effect" is the first historical evidence that cancer cells can adjust their metabolism in order to promote cell growth. Indeed, the increased glucose uptake and metabolism that underlie the Warburg effect are now considered as one of the hallmarks of cancer [32]. Purinergic signaling is a cellular communication pathway mediated by extracellular nucleotides and nucleosides [33]. The nucleoside adenosine has crucial roles in the regulation of purine biosynthesis, gene translation, and the fate of RNA [34]. Purines are components of nucleic acids and have important physiological functions as intracellular and extracellular signaling molecules. Purine metabolites, especially uric acid, are associated with congenital and complex diseases [35]. It has been shown that cellular metabolism is disrupted in RCC tumors, and that changes in purine metabolism are associated with the poor survival of RCC patients [36]. In the present study, KIRC were clustered according to purine genes, and a purine-related, differential lncRNA risk score (Purine Score) was developed to predict the outcome of KIRC patients. We found that age, N, and M were independent prognostic factors for KIRC patients.

RCC is one of the most heavily immune-infiltrated tumors [37,38], and the immune response is a critical factor in the occurrence and treatment of KIRC [39]. Emerging evidence suggests that activation of specific metabolic pathways may play a role in regulating angiogenesis and inflammatory signatures [40,41]. Features of the TME may also strongly affect disease biology and the response to systemic therapy [42–45]. Therefore, identifying the cells of origin for RCC, as well as novel cell types within the TME, are very important for the development of targeted therapies [46]. In the current research we therefore investigated the relationship between Purine Score and cellular components or immune responses. An abnormal immune cell response was associated with survival models (T, N, M, stage, gender, age, and status). A correlation was found between Purine Score and abnormal expression of immune checkpoint genes. Phenotypic variation can be observed as intratumoral heterogeneity, which leads to genomic instability resulting in mutations, somatic copy number alterations, and epigenomic changes [47]. The heterogeneity observed between RCC subtypes is related to significant differences in tumor invasiveness and the risk of metastatic disease [48]. Most clear cell carcinomas (sporadic and familial) are associated with mutations and deletions of the *VHL* gene on 3p.25, as well as other nearby genes (*SETD2*, *BAP1*, *PBRM1*) [49,50]. In this study, we found mutations in *TP53*, *TRIOBP*, *PBRM1*, *PKHD1*, *VHL*, *NPHP3*, *TLN2*, *CABIN1*, *ABCC6*, *XIRP2* and *CHD4*. Deletion of these tumor suppressor genes may play a role in the development of KIRC and affect the clinical course of this disease.

Molecular characterization of RCC helps to identify driver genes and specific molecular pathways, as well as the characterization of TME, thereby enhancing our understanding of this cancer type [51]. Aberrant expression of lncRNAs is closely associated with various diseases, such as the occurrence and development of cancers [52]. It has been reported that ferroptosis-related lncRNAs could accurately predict the outcome of KIRC [53]. A prognostic signature of angiogenesis-associated gene-related lncRNAs shows promise as an independent prognostic indicator for KIRC patients [54]. Moreover, previous studies have suggested that *LINC01671* may be a useful indicator for clinical stratification management and treatment decision-making in lung adenocarcinoma patients [55,56]. Su *et al.* [57] reported that *LINC01671* is a protective gene in clear cell RCC (hazard ratio $<1$). *LINC01671* was found to be significantly associated with OS using multivariate Cox regression, which is the first report that *LINC01671* has been associated with clear cell RCC in their study. However, research on *LINC01671* in KIRC is limited. In our study, our bioinformatics analysis also showed that *LINC01671* has a hazard ratio $<1$, indicating that *LINC01671* is a protective gene. Survival analysis revealed that patients with high expression of *LINC01671* have a higher survival rate, suggesting that *LINC01671* has a positive impact on the prognosis of KIRC. Furthermore, *in vitro* experiments revealed that interfering with *LINC01671* promoted proliferation and migration of 786-O cells while suppressing apoptosis. Overexpression of *LINC01671* inhibited proliferation and migration of CAKI-1 cells while promoting apoptosis. Therefore, our results provide evidence that *LINC01671* is a protective gene in KIRC and enrich our understanding of its regulatory role in cancer. Further analysis sug-

gested that *LINC01671* can positively regulate the MAPK, NF-kappa B, mTOR, PI3K-Akt, and Wnt signaling pathways. However, the specific cellular mechanisms involving *LINC01671* require further study.

## 5. Conclusions

In summary, purine metabolism-related *LINC01671* plays an important role in the development, progression and prognosis of KIRC. We constructed a purine-related, differential lncRNA risk score model (Purine Score) that can predict the survival of KIRC patients with high accuracy. This study has identified new candidate genes for the treatment of KIRC patients.

## Availability of Data and Materials

The datasets used and analyzed during the current study are available from the corresponding author on reasonable request.

## Author Contributions

WY contributed to conceptualization, data curation, validation, writing of the original draft and funding acquisition. JHW, YML, KHL and YC contributed to formal analysis, investigation, software and methodology. YSC contributed to conceptualization, funding acquisition, project administration, supervision, and review. All authors contributed to editorial changes in the manuscript. All authors read and approved the final manuscript. All authors have participated sufficiently in the work to take public responsibility for appropriate portions of the content and agreed to be accountable for all aspects of the work in ensuring that questions related to its accuracy or integrity.

## Ethics Approval and Consent to Participate

Not applicable.


## Acknowledgment

Not applicable.

## Funding

This work was supported by the Hunan Clinical Research Center for Chronic Kidney Disease (No. 2019SK4009), the Natural Science Foundation of Hunan Province (No. 2021JJ40290), the Hunan Provincial Department of Education (No. 22C0034), the Hunan Provincial Department of Education (No. 21B0038), the Doctoral Fund and 2020 national self-cultivation project (No. BSJJ202006), and the Natural Science Foundation of Hunan Province (No. 2023JJ60454).


## Conflict of Interest

The authors declare no conflict of interest.

## Supplementary Material

Supplementary material associated with this article can be found, in the online version, at https://doi.org/10.31083/j.fbl2812354.

## References


[1] Hsieh JJ, Purdue MP, Signoretti S, Swanton C, Albiges L, Schmidinger M, *et al*. Renal cell carcinoma. Nature Reviews. Disease Primers. 2017; 3: 17009.

[2] Zhang Z, Zhang Y, Zhang R. P4HA3 promotes clear cell renal cell carcinoma progression via the PI3K/AKT/GSK3$\beta$ pathway. Medical Oncology (Northwood, London, England). 2023; 40: 70.

[3] Nguyen TTM, Nguyen TH, Kim HS, Dao TTP, Moon Y, Seo M, *et al*. GPX8 regulates clear cell renal cell carcinoma tumorigenesis through promoting lipogenesis by NNMT. Journal of Experimental & Clinical Cancer Research: CR. 2023; 42: 42.

[4] Qiu J, Wang Z, Xu Y, Zhao L, Zhang P, Gao H, *et al*. Low expression of SLC34A1 is associated with poor prognosis in clear cell renal cell carcinoma. BMC Urology. 2023; 23: 45.

[5] Xu J, Wang Y, Jiang J, Yin C, Shi B. ADAM12 promotes clear cell renal cell carcinoma progression and triggers EMT via EGFR/ERK signaling pathway. Journal of Translational Medicine. 2023; 21: 56.

[6] Wolf MM, Kimryn Rathmell W, Beckermann KE. Modeling clear cell renal cell carcinoma and therapeutic implications. Oncogene. 2020; 39: 3413–3426.

[7] Huang Y, Sun H, Guo P. Research Progress of Tumor Microenvironment Targeted Therapy for Clear Cell Renal Cell Carcinoma. Cancer Control: Journal of the Moffitt Cancer Center. 2023; 30: 10732748231155700.

[8] Yang B, Zhang L, Cao Y, Chen S, Cao J, Wu D, *et al*. Overexpression of lncRNA IGFBP4-1 reprograms energy metabolism to promote lung cancer progression. Molecular Cancer. 2017; 16: 154.

[9] Liu J, Hong S, Yang J, Zhang X, Wang Y, Wang H, *et al*. Targeting purine metabolism in ovarian cancer. Journal of Ovarian Research. 2022; 15: 93.

[10] Chua SM, Fraser JA. Surveying purine biosynthesis across the domains of life unveils promising drug targets in pathogens. Immunology and Cell Biology. 2020; 98: 819–831.

[11] Furuhashi M. New insights into purine metabolism in metabolic diseases: role of xanthine oxidoreductase activity. American Journal of Physiology. Endocrinology and Metabolism. 2020; 319: E827–E834.

[12] Daignan-Fornier B, Pinson B. Yeast to Study Human Purine Metabolism Diseases. Cells. 2019; 8: 67.

[13] Yin J, Ren W, Huang X, Deng J, Li T, Yin Y. Potential Mechanisms Connecting Purine Metabolism and Cancer Therapy. Frontiers in Immunology. 2018; 9: 1697.

[14] Jackson RC, Goulding FJ, Weber G. Enzymes of purine metabolism in human and rat renal cortex and renal cell carcinoma. Journal of the National Cancer Institute. 1979; 62: 749–754.

[15] Hao L, Wu W, Xu Y, Chen Y, Meng C, Yun J, *et al*. LncRNA-MALAT1: A Key Participant in the Occurrence and Development of Cancer. Molecules (Basel, Switzerland). 2023; 28: 2126.

[16] Jung HJ, Kim HJ, Park KK. Potential Roles of Long Noncoding RNAs as Therapeutic Targets in Renal Fibrosis. International Journal of Molecular Sciences. 2020; 21: 2698.

[17] Shen H, Luo G, Chen Q. Long noncoding RNAs as tumorigenic factors and therapeutic targets for renal cell carcinoma. Cancer Cell International. 2021; 21: 110.

[18] Yang J, Wang K, Yang Z. Treatment strategies for clear cell renal cell carcinoma: Past, present and future. Frontiers in Oncology. 2023; 13: 1133832.
[19] Lai Y, Tang F, Huang Y, He C, Chen C, Zhao J, *et al*. The tumour microenvironment and metabolism in renal cell carcinoma targeted or immune therapy. Journal of Cellular Physiology. 2021; 236: 1616–1627.
[20] Bui TO, Dao VT, Nguyen VT, Feugeas JP, Pamoukdjian F, Bousquet G. Genomics of Clear-cell Renal Cell Carcinoma: A Systematic Review and Meta-analysis. European Urology. 2022; 81: 349–361.
[21] An Y, Duan H. The role of m6A RNA methylation in cancer metabolism. Molecular Cancer. 2022; 21: 14.
[22] di Meo NA, Lasorsa F, Rutigliano M, Milella M, Ferro M, Battaglia M, *et al*. The dark side of lipid metabolism in prostate and renal carcinoma: novel insights into molecular diagnostic and biomarker discovery. Expert Review of Molecular Diagnostics. 2023; 23: 297–313.
[23] Lucarelli G, Loizzo D, Franzin R, Battaglia S, Ferro M, Cantiello F, *et al*. Metabolomic insights into pathophysiological mechanisms and biomarker discovery in clear cell renal cell carcinoma. Expert Review of Molecular Diagnostics. 2019; 19: 397–407.
[24] di Meo NA, Lasorsa F, Rutigliano M, Loizzo D, Ferro M, Stella A, *et al*. Renal Cell Carcinoma as a Metabolic Disease: An Update on Main Pathways, Potential Biomarkers, and Therapeutic Targets. International Journal of Molecular Sciences. 2022; 23: 14360.
[25] De Marco S, Torsello B, Minutiello E, Morabito I, Grasselli C, Bombelli S, *et al*. The cross-talk between Abl2 tyrosine kinase and TGF$\beta$1 signalling modulates the invasion of clear cell Renal Cell Carcinoma cells. FEBS Letters. 2023; 597: 1098–1113.
[26] Bianchi C, Meregalli C, Bombelli S, Di Stefano V, Salerno F, Torsello B, *et al*. The glucose and lipid metabolism reprogramming is grade-dependent in clear cell renal cell carcinoma primary cultures and is targetable to modulate cell viability and proliferation. Oncotarget. 2017; 8: 113502–113515.
[27] Ragone R, Sallustio F, Piccinonna S, Rutigliano M, Vanessa G, Palazzo S, *et al*. Renal Cell Carcinoma: A Study through NMR-Based Metabolomics Combined with Transcriptomics. Diseases (Basel, Switzerland). 2016; 4: 7.
[28] Lucarelli G, Galleggiante V, Rutigliano M, Sanguedolce F, Cagiano S, Bufo P, *et al*. Metabolomic profile of glycolysis and the pentose phosphate pathway identifies the central role of glucose-6-phosphate dehydrogenase in clear cell-renal cell carcinoma. Oncotarget. 2015; 6: 13371–13386.
[29] Lucarelli G, Rutigliano M, Sallustio F, Ribatti D, Giglio A, Lepore Signorile M, *et al*. Integrated multi-omics characterization reveals a distinctive metabolic signature and the role of NDUFA4L2 in promoting angiogenesis, chemoresistance, and mitochondrial dysfunction in clear cell renal cell carcinoma. Aging. 2018; 10: 3957–3985.
[30] Bombelli S, Torsello B, De Marco S, Lucarelli G, Cifola I, Grasselli C, *et al*. 36-kDa Annexin A3 Isoform Negatively Modulates Lipid Storage in Clear Cell Renal Cell Carcinoma Cells. The American Journal of Pathology. 2020; 190: 2317–2326.
[31] Lucarelli G, Rutigliano M, Loizzo D, di Meo NA, Lasorsa F, Mastropasqua M, *et al*. MUC1 Tissue Expression and Its Soluble Form CA15-3 Identify a Clear Cell Renal Cell Carcinoma with Distinct Metabolic Profile and Poor Clinical Outcome. International Journal of Molecular Sciences. 2022; 23: 13968.
[32] Shaw RJ. Glucose metabolism and cancer. Current Opinion in Cell Biology. 2006; 18: 598–608.
[33] Savio LEB, Leite-Aguiar R, Alves VS, Coutinho-Silva R, Wyse ATS. Purinergic signaling in the modulation of redox biology. Redox Biology. 2021; 47: 102137.
[34] Srinivasan S, Torres AG, Ribas de Pouplana L. Inosine in Biology and Disease. Genes. 2021; 12: 600.
[35] Nelson KL, Voruganti VS. Purine metabolites and complex diseases: role of genes and nutrients. Current Opinion in Clinical Nutrition and Metabolic Care. 2021; 24: 296–302.
[36] Popławski P, Tohge T, Bogusławska J, Rybicka B, Tański Z, Treviño V, *et al*. Integrated transcriptomic and metabolomic analysis shows that disturbances in metabolism of tumor cells contribute to poor survival of RCC patients. Biochimica et Biophysica Acta. Molecular Basis of Disease. 2017; 1863: 744–752.
[37] Vuong L, Kotecha RR, Voss MH, Hakimi AA. Tumor Microenvironment Dynamics in Clear-Cell Renal Cell Carcinoma. Cancer Discovery. 2019; 9: 1349–1357.
[38] Tamma R, Rutigliano M, Lucarelli G, Annese T, Ruggieri S, Cascardi E, *et al*. Microvascular density, macrophages, and mast cells in human clear cell renal carcinoma with and without bevacizumab treatment. Urologic Oncology. 2019; 37: 355.e11–355.e19.
[39] Xu WH, Xu Y, Wang J, Wan FN, Wang HK, Cao DL, *et al*. Prognostic value and immune infiltration of novel signatures in clear cell renal cell carcinoma microenvironment. Aging. 2019; 11: 6999–7020.
[40] Netti GS, Lucarelli G, Spadaccino F, Castellano G, Gigante M, Divella C, *et al*. PTX3 modulates the immunoflogosis in tumor microenvironment and is a prognostic factor for patients with clear cell renal cell carcinoma. Aging. 2020; 12: 7585–7602.
[41] Lucarelli G, Rutigliano M, Ferro M, Giglio A, Intini A, Triggiano F, *et al*. Activation of the kynurenine pathway predicts poor outcome in patients with clear cell renal cell carcinoma. Urologic Oncology. 2017; 35: 461.e15–461.e27.
[42] Lasorsa F, di Meo NA, Rutigliano M, Milella M, Ferro M, Pandolfo SD, *et al*. Immune Checkpoint Inhibitors in Renal Cell Carcinoma: Molecular Basis and Rationale for Their Use in Clinical Practice. Biomedicines. 2023; 11: 1071.
[43] Ghini V, Laera L, Fantechi B, Monte FD, Benelli M, McCartney A, *et al*. Metabolomics to Assess Response to Immune Checkpoint Inhibitors in Patients with Non-Small-Cell Lung Cancer. Cancers. 2020; 12: 3574.
[44] Lucarelli G, Netti GS, Rutigliano M, Lasorsa F, Loizzo D, Milella M, *et al*. MUC1 Expression Affects the Immunoflogosis in Renal Cell Carcinoma Microenvironment through Complement System Activation and Immune Infiltrate Modulation. International Journal of Molecular Sciences. 2023; 24: 4814.
[45] Lasorsa F, Rutigliano M, Milella M, Ferro M, Pandolfo SD, Crocetto F, *et al*. Cellular and Molecular Players in the Tumor Microenvironment of Renal Cell Carcinoma. Journal of Clinical Medicine. 2023; 12: 3888.
[46] Schreibing F, Kramann R. Mapping the human kidney using single-cell genomics. Nature Reviews. Nephrology. 2022; 18: 347–360.
[47] Bailey C, Black JRM, Reading JL, Litchfield K, Turajlic S, McGranahan N, *et al*. Tracking Cancer Evolution through the Disease Course. Cancer Discovery. 2021; 11: 916–932.
[48] Garje R, Elhag D, Yasin HA, Acharya L, Vaena D, Dahmoush L. Comprehensive review of chromophobe renal cell carcinoma. Critical Reviews in Oncology/hematology. 2021; 160: 103287.
[49] Akhtar M, Al-Bozom IA, Al Hussain T. Molecular and Metabolic Basis of Clear Cell Carcinoma of the Kidney. Advances in Anatomic Pathology. 2018; 25: 189–196.
[50] Mitchell TJ, Rossi SH, Klatte T, Stewart GD. Genomics and clinical correlates of renal cell carcinoma. World Journal of Urology. 2018; 36: 1899–1911.
[51] Beksac AT, Paulucci DJ, Blum KA, Yadav SS, Sfakianos JP, Badani KK. Heterogeneity in renal cell carcinoma. Urologic Oncology. 2017; 35: 507–515.
[52] Bhan A, Soleimani M, Mandal SS. Long Noncoding RNA and Cancer: A New Paradigm. Cancer Research. 2017; 77: 3965–

3981.
[53] Xing XL, Yao ZY, Ou J, Xing C, Li F. Development and validation of ferroptosis-related lncRNAs prognosis signatures in kidney renal clear cell carcinoma. Cancer Cell International. 2021; 21: 591.
[54] Zhang W, Liu Z, Wang J, Geng B, Hou W, Zhao E, *et al*. The clinical significance, immune infiltration, and tumor mutational burden of angiogenesis-associated lncRNAs in kidney renal clear cell carcinoma. Frontiers in Immunology. 2022; 13: 934387.
[55] Geng W, Lv Z, Fan J, Xu J, Mao K, Yin Z, *et al*. Identification of the Prognostic Significance of Somatic Mutation-Derived LncRNA Signatures of Genomic Instability in Lung Adenocarcinoma. Frontiers in Cell and Developmental Biology. 2021; 9: 657667.
[56] Yang L, Guo G, Yu X, Wen Y, Lin Y, Zhang R, *et al*. Mutation-Derived Long Noncoding RNA Signature Predicts Survival in Lung Adenocarcinoma. Frontiers in Oncology. 2022; 12: 780631.
[57] Su BC, Xu SH, Yang SF, Ye XD, Song YW, Huang ZX. LINC00839, LINC01671, AC093673 and AC008760 are Associated with the Prognosis and Immune Infiltration of Clear-cell Renal Cell Carcinoma. Current Proteomics. 2023; 20: 39–50.